Sliding Mode Control Design of a Two-Wheel Inverted Pendulum Robot: Simulation, Design and Experiments

Mikail S. Arani, Hamid Ebrahimi Orimi, Wen-Fang Xie and Henry Hong

Abstract The current paper investigates a sliding mode controller for stabilizing a two-wheel inverted pendulum (TWIP) robot. It is well-known that the controller in the mobile robot plays a critical role in self-balancing and stabilizing. The TWIP robot has two DC gear motors with a high-resolution encoder and zero backlash, but with friction. It is a highly nonlinear and unstable system, which poses challenges for controller design. In this study, a mathematical dynamic model is built using Lagrangian function method. And a sliding mode controller (SMC) is proposed for auto-balancing and yaw rotation. A gyro and an accelerometer are adopted to measure the pitch angle and pitch rate. The effect on the sensors installation location was analyzed and compensated, and the precision of the pose estimation is improved accordingly. A comparison of the proposed SMC controller with proportional-integral-derivative (PID) controller and state feedback controller (SFC) with linear quadratic regulation (LQR) has been conducted. The experimental test results demonstrate the SMC controller outperforms PID controller, SFC and SMC controller in Zhang and Li (Proceedings of 35th Chinese control conference (CCC). IEEE) [14] in terms of transient performance and disturbance rejection ability.

Keywords PID controller · State feedback controller (SFC) · Linear quadratic regulator (LQR) · Sensor data fusion · Sliding mode control (SMC) · Two-wheel inverted pendulum (TWIP) robot

1 Introduction

In recent years, self-balancing robots have attracted increasing attention in both industry and academia, since designing and testing control algorithms become more achievable with the rapid development of microcontrollers. Two-wheeled inverted

M. S. Arani · H. Ebrahimi Orimi · W.-F. Xie (✉) · H. Hong
Department of Mechanical Industrial & Aerospace Engineering,
Concordia University, Montreal, QC, Canada
e-mail: wfxie@encs.concordia.ca

F. Janabi-Sharifi and W. Melek (eds.), *Advances in Motion Sensing and Control for Robotic Applications*, Lecture Notes in Mechanical Engineering,
https://doi.org/10.1007/978-3-030-17369-2_7

pendulum (TWIP) robots have become more and more popular due to its light weight, small footprint, rapid rotation and high maneuverability. One of the applications of using these robots can be a service robot platform like Segway. However, the inherent instability and nonlinearity of the TWIP requires a sophisticated control scheme.

PID is a commonly used non-model based control method for self-balancing robot, as there is no need to build the mathematics model. The three parameters can be tuned by trial and error or by experience. Although PID owns some robustness to disturbance and uncertainties to a certain extent, it cannot handle the sudden, large disturbance and modeling error [1]. Moreover, it is not a trivial task to obtain the optimized gains of PID controller. Recently, the soft computing techniques such as fuzzy logic and neural networks have been used to control TWIP robot [2, 3]. Two fuzzy controllers based on Mamdani and Takagi-Sugeno are designed for an inverted pendulum subjected to disturbance. Moreover, an artificial neural network-based real-time switching dynamic controller is designed to solve balancing problem on various loose surfaces such as sand, pebble and soil [4]. A visual robot control interface is developed in C++ software development environment so that robot controller parameters can be changed as desired.

Recently, the model-based control of TWIP has been proposed to deal with the nonlinearity and disturbance. The state feedback controller with optimized control gains is one of the mostly used methods in the practical systems [5]. In [6], a linear SFC has been designed based on the linearized model, which needs very accurate dynamic models of the robots. Hence, the optimized SFC can only work in the certain operating range and cannot deal with system uncertainty. When the operating point is changed, the control gains have to be re-tuned in order to stabilize the robot, which is not very practical in the operation [7]. Due to the nonlinearity of the systems, the linear controllers such as PID and state feedback controllers do not react efficiently, therefore, some researchers concentrate on the design of nonlinear controllers such as robust feedback [8], back stepping [9], feedback linearization [10, 11] and sliding mode controllers (SMC) [12, 13] to provide effective reaction to the uncertainties and disturbance for TWIP robots. All these mentioned controllers [8–13] are only validated through simulation and no experimental tests of these controllers have been carried out on real TWIP robots.

Among these nonlinear controllers, SMC is known to have a good robustness to the model uncertainties and disturbance. It can deal with the nonlinear unstable system with easy implementation, insensitivity to parameters variation and quick response independence of external disturbances. SMC has been successfully used for controlling the TWIP robot. In [14–16], the SMC controllers are designed based on 2 degree-of-freedom (DoF) linear dynamic model of TWIP and are tested in the real robots. In [3], the authors design a backstepping sliding mode controller for a TWIP robot and validate the trajectory tracking performance in a real TWIP. However, the control design combines the backstepping and sliding mode controller and focuses on trajectory tracking. The combination increases the complexity of implementation on the real robots and the robustness of controller has not been demonstrated. The goal of the current study is to provide an effective SMC control design, which is

easy for implementation on a real robot and has a good robustness for dealing with uncertainties and sudden disturbance.

In this paper, such a SMC controller has been designed and implemented on a TWIP robot. First, a 3-DoF dynamic model of a customer built TWIP robot is derived by using Lagrangian function method. The robot is composed of two gear DC motors driving two wheels, a structure, battery, sensors and controller. It is a highly nonlinear and unstable system. Then, based on the built nonlinear model, a SMC with easy implementation has been designed for balancing and stabilizing the robot. Simulation tests have been carried out to compare the proposed SMC with PID controller and state feedback controller (SFC) tuned by LQR. The experimental results demonstrate the superiority of SMC controller to the other controllers including PID, SFC and SMC in [14] in terms of transient performance and disturbance rejection capability.

The paper is organized as follows. The paper begins with an introduction and the next section provides a 3-DOF dynamic of the model of the TWIP robot built in our lab. In Sect. 3, the PID, SFC and SMC are designed and the simulation results of both controllers are presented. Section 4 presents the experiment results of three controllers and comparison with the SMC in [14]. The conclusion is drawn in Sect. 5.

2 Dynamics Modelling

The TWIP robot is built in our lab to serve as test platform for various controllers. In order to control this type of unstable robot effectively, the first step is to model the robots dynamic behavior in the yaw and pitch motions. The schematic diagram of the TWIP robot is shown in Fig. 1 and the parameters' description has been provided in Table 1.

The dynamic model of the robot is built based on the Lagrangian function method [17]. Equation (1) presents Lagrangian where L_1, L_2 and B are translation kinematic energy, rotational kinematic energy and potential energy, respectively.

$$L_a = L_1 + L_2 + B \tag{1}$$

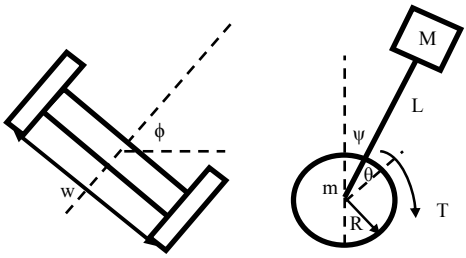

Fig. 1 Schematic diagram of the TWIP robot

Table 1 Parameters of two wheeled inverted pendulum

Parameters	Unit	Description	Parameters	Unit	Description
$W = 0.242$	m	Body width	$J_\psi = \frac{ML^2}{2}$	kgm^2	Body pitch inertia moment
$M = 1.047$	kg	Body mass	$J_\phi = \frac{M(W^2+D^2)}{12}$	kgm^2	Body yaw inertia moment
$m = 0.118$	kg	Wheels mass	$R_m = 1.900$	Ω	DC motor resistance
$R = 0.060$	m	Diameter of wheel	$K_t = 13.400$	mNm/A	DC motor torque constant
$g = 9.810$	m/s^2	Gravity acceleration	$K_b = 1.400$	mv/rpm	DC motor back E.M.F constant
$L = 0.030$	m	Distance between the center of the mass and the Wheel axle	$fm = 0.0022$		Friction coefficient between body and DC motor
$D = 0.050$	m	Body depth	θ, ψ, ϕ	rad	Rotary angle of the wheel, pitch angle and yaw angle of the robot
$n = 64{:}1$	–	Gear ratio	l, r, b	–	Subscripts indicating left or right wheels and the robot body, respectively
$J_w = \frac{mR^2}{2}$	kgm^2	Wheel inertia moment			

It is assumed that the robot has 3 degree of freedoms (DOFs). The generalized variables of the robot are angle of the wheel (θ), pitch angle (ϕ) and yaw angle (ψ) [17]. According to the robot dynamics, the translational and rotational kinetic energies are described as follows (Eqs. 2–4):

$$L_1 = \frac{1}{2}m\left(\dot{x}_l^2 + \dot{y}_l^2\right) + \frac{1}{2}m\left(\dot{x}_r^2 + \dot{y}_r^2\right) + \frac{1}{2}M\left(\dot{x}_b^2 + \dot{y}_b^2 + \dot{z}_b^2\right) \tag{2}$$

$$L_2 = \frac{1}{2}J_w\dot{\theta}_l^2 + \frac{1}{2}J_w\dot{\theta}_r^2 + \frac{1}{2}J_\psi\dot{\psi}^2 + \frac{1}{2}J_\phi\dot{\phi}^2 + \frac{1}{2}n^2J_m\left(\dot{\theta}_l - \dot{\psi}\right)^2 + \frac{1}{2}n^2J_m\left(\dot{\theta}_r - \dot{\psi}\right)^2 \tag{3}$$

$$B = Mgz_b \tag{4}$$

The Lagrangian equations (5–7) are:

$$\frac{d}{dl}\left(\frac{\partial L_a}{\partial \dot{\theta}}\right) - \frac{\partial L_a}{\partial \theta} = F_l + F_r \tag{5}$$

$$\frac{d}{dl}\left(\frac{\partial L_a}{\partial \dot{\psi}}\right) - \frac{\partial L_a}{\partial \psi} = -F_l - F_r \tag{6}$$

$$\frac{d}{dl}\left(\frac{\partial L_a}{\partial \dot{\phi}}\right) - \frac{\partial L_a}{\partial \phi} = \frac{W}{2R}(F_r - F_l) \tag{7}$$

where, F_l and F_r are the torques on the left and right wheels, respectively. Moreover, they could be defined as (8) and (9):

$$F_l = nK_t i_l \tag{8}$$

$$F_r = nK_t i_r \tag{9}$$

By substituting the kinetic and potential energies in the Lagrangian equations, the equations of motion are as follows:

$$\left((2m+M)R^2 + 2J_w + 2n^2J_m\right)\ddot{\theta} + \left(MRL\cos\psi - 2n^2J_m\right)\ddot{\psi} - MLR\psi^2\sin\psi = F_\theta \tag{10}$$

$$\left(MRL\cos\psi - 2n^2J_m\right)\ddot{\theta} + \left(ML^2 + J_\psi + 2n^2J_m\right)\ddot{\psi} - MgL\sin\psi - ML^2\dot{\phi}^2\sin\psi\cos\psi = F_\psi \tag{11}$$

$$\left(\frac{1}{2}mW^2 + J_\phi + \frac{W^2}{2R^2}\left(J_w + n^2J_m\right) + ML^2\sin^2\psi\right)\ddot{\phi} + 2ML^2\dot{\psi}\dot{\phi}\sin\psi\cos\psi = F_\phi \tag{12}$$

In which the external forces can be presented as Eqs. 13–15:

$$F_\theta = \frac{nK_t}{R_m}(v_l + v_r) + 2\left(\frac{n^2K_tK_b}{R_m}\right)\dot{\psi} - 2\left(\frac{n^2K_tK_b}{R_m}\right)\dot{\theta} \tag{13}$$

$$F_\psi = -\frac{nK_t}{R_m}(v_l + v_r) - 2\left(\frac{n^2K_tK_b}{R_m}\right)\dot{\psi} + 2\left(\frac{n^2K_tK_b}{R_m}\right)\dot{\theta} \tag{14}$$

$$F_\phi = \frac{nK_tW}{2RR_m}(v_r - v_l) - \frac{\mathrm{W}^2}{2R^2}\left(\frac{n^2K_tK_b}{2R_m}\right)\dot{\phi} \tag{15}$$

The aforementioned equations can be transformed to nonlinear state space, by defining (16):

$$\left[\theta, \dot{\theta}, \psi, \dot{\psi}, \phi, \dot{\phi}\right] \tag{16}$$

As the state variables (17):

$$X = [x_1, x_2, x_3, x_4, x_5, x_6] = \left[\theta, \dot{\theta}, \psi, \dot{\psi}, \phi, \dot{\phi}\right] \tag{17}$$

Hence, the general form of the state space is given as Eqs. 18–21:

$$M(x)\dot{x} = f(x) + u \tag{18}$$

where:

$$M(x) = \begin{bmatrix} 1 & 0 & 0 & 0 & 0 & 0 \\ M_{21} & M_{22} & -M_{24} & M_{24} & 0 & 0 \\ 0 & 0 & 1 & 0 & 0 & 0 \\ -M_{21} & M_{24} & M_{21} & M_{44} & 0 & 0 \\ 0 & 0 & 0 & 0 & 1 & 0 \\ 0 & 0 & 0 & 0 & M_{65} & M_{66} \end{bmatrix} \tag{19}$$

$$f(x) = \begin{bmatrix} f_1 \\ f_2 \\ f_3 \\ f_4 \\ f_5 \\ f_6 \end{bmatrix} = \begin{bmatrix} x_2 \\ MLRx_4^2 \sin x_3 \\ x_4 \\ MgL \sin x_3 + ML^2 x_6^2 \sin x_3 \cos x_3 \\ x_6 \\ -2ML^2 x_4 x_6 \sin x_3 \cos x_3 \end{bmatrix} \tag{20}$$

$$u = \begin{bmatrix} 0 \\ u_2 \\ 0 \\ -u_2 \\ 0 \\ u_6 \end{bmatrix} = \begin{bmatrix} 0 & 0 \\ \frac{nK_t}{R_m} & \frac{nK_t}{R_m} \\ 0 & 0 \\ -\frac{nK_t}{R_m} & -\frac{nK_t}{R_m} \\ 0 & 0 \\ \frac{nK_t w}{2RR_m} & -\frac{nK_t w}{2RR_m} \end{bmatrix} \begin{bmatrix} v_r \\ v_l \end{bmatrix} \tag{21}$$

where u is the control input which is generated by the controllers in this study.

3 Controllers Design

3.1 PID Controller

To stabilize the two-wheel inverted pendulum, the proportional-integrator-derivative (PID) controllers have been designed with following transfer function:

$$G_c = K_P + K_D s + \frac{K_I}{s} \tag{22}$$

Two PID controllers in parallel are designed. The first PID controller aims at regulating the body pitch angle. The second PID controller aims at regulating the angular position of the wheels [18, 19].

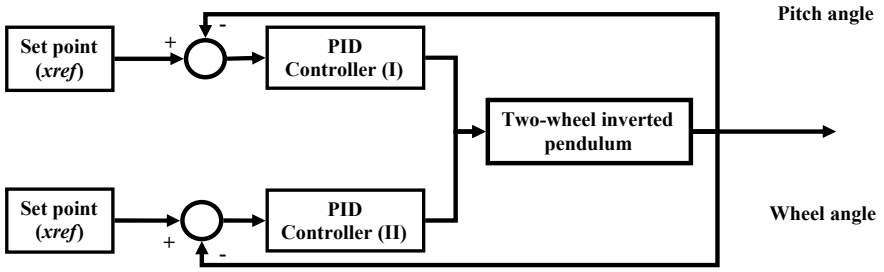

Fig. 2 TWIP closed loop block diagram having PID controller

Table 2 PID controller parameters

	K_p	K_I	K_D
Ψ	5.19	0.009	0.00045
θ	5.50	0.00078	0.00025

There are two measurements of the angle from two different sources. The measurement from accelerometer gets affected by sudden horizontal movements (it could be used to measure the Ψ) and the measurement from gyroscope gradually drifts away from actual value (it could be used to measure θ). In other words, the accelerometer reading gets affected by short duration signals and the gyroscope reading is affected by long duration signals. To stabilize the robot, two PID controllers work simultaneously to control pitch and wheel angles which are measured by accelerometer and gyroscope, respectively.

The PID controller has been applied to the simulated model which has been presented in the Eq. 22. Figure 2 is the block diagram of closed-loop position control for the TWIP. The parameters of the PID controllers are obtained by trial and error. The tuned parameters are given as in Table 2.

In Fig. 2, *xref* represents the desired states and we set $xref = 0\ rad$ to stabilize the TWIP.

The simulation of the closed-loop PID controller has been done in SIMULINK using ode45 method with variable time step. As shown in Fig. 3, two different initial pinch angles have been provided to evaluate the performance of PID controllers.

3.2 SFC Designed by LQR

To stabilize the two-wheel inverted pendulum, the optimal SFC have been designed using LQR. Equation (23) is the linear quadratic regulator objective function:

$$J = \int_0^\infty [x^T(t)Qx(t) + u^T(t)Ru(t)]dt \tag{23}$$

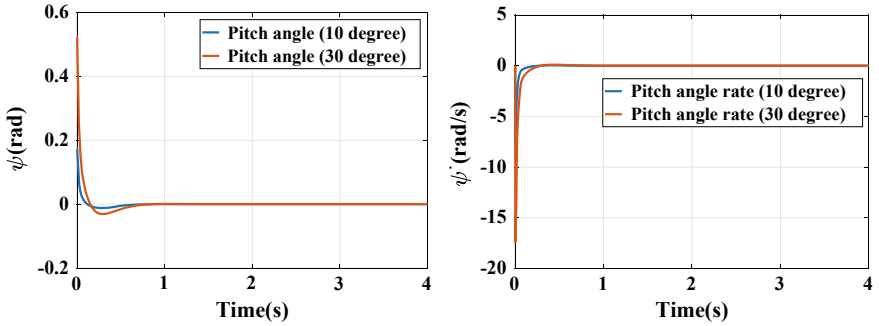

Fig. 3 The pitch angle and its rate of PID controller in simulation

The optimal control input which minimizes the above objective function (23) is presented in (24):

$$u(t) = -Kx(t) \ where \ K = R^{-1}B^T P \tag{24}$$

Matrix P can be obtained by solving Riccati Eq. (25):

$$A^T P + PA - PBR^{-1}B^T P + C^T C = 0 \tag{25}$$

where A, B and C are state space matrices. Two optimal LQRs have been designed for left and right DC motors.

To stabilize the robot, two state feedback controllers work simultaneously to control the states of DC motors.

The state feedback controller has been applied to the simulated model which has been presented in the Eq. 24. Figure 4 is the block diagram of closed-loop states control for the TWIP. The gains details are given as in Table 3.

Table 3 SFC gains

	$[k_1, k_2, k_3, k_4, k_5, k_6]$
Left motor	$[-0.7071, -0.3078, -11.3966, -1.6791, 0.0000, 0.2118]$
Right motor	$[-0.7071, -0.3078, -11.3966, -1.6791, 0.0000, -0.2118]$

xref: It represents the desired states, in this case to stabilize the TWIP the $xref = 0$ rad (Fig. 4).

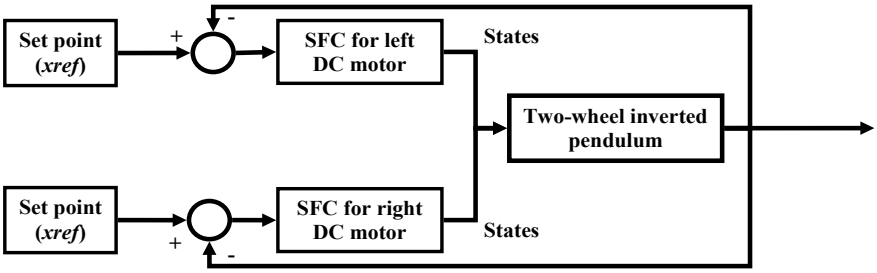

Fig. 4 TWIP closed-loop block diagram with SFCs

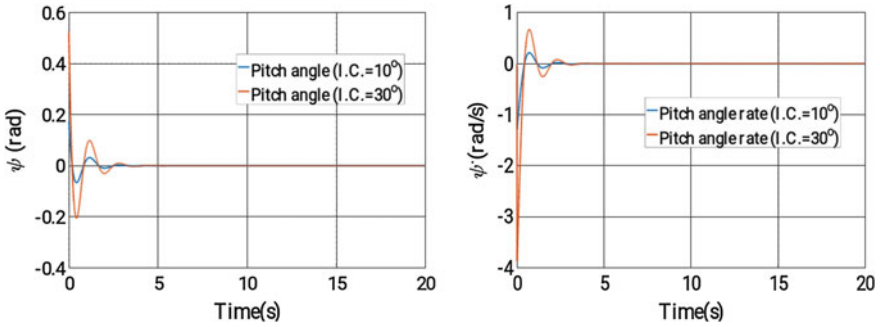

Fig. 5 The pitch angle and its rate of SFC in simulation

The simulation of the closed-loop SFC has been done in SIMULINK using ode45 method with variable time step. As shown in Fig. 5, two different initial pinch angles have been provided to evaluate the performance of SFC.

3.3 SMC

As the yaw motion and self-balancing of the robot need to be controlled properly, a sliding mode control is proposed and designed to achieve self-balancing and stabilizing. Due to the system's nonlinearity and uncertainty, SFC could not precisely balance the pendulum and reject the large disturbance within short time period. Hence, the sliding mode controller is designed to handle the nonlinearity of the system using the sliding surface approach.

The design of the wheel angle sliding mode controller is presented as follows:

$$s_1 = c_1\psi + c_2\dot{\psi} \tag{26}$$

$$\dot{s}_1 = -\varepsilon_1 sign(s_1) \tag{27}$$

$$u_2 = \frac{c_1\left(M_{24}^2 - M_{22}M_{44}\right)\dot{\psi} + \left(M_{24}^2 + M_{22}M_{44}\right)\varepsilon_1 sign(s_1)}{c_2(-M_{24} - M_{22})} + \frac{c_2M_{24}f_2 - c_2M_{22}f_4}{c_2(-M_{24} - M_{22})} + \frac{c_2M_{12}(-M_{24} + M_{22})\dot{\theta} - c_2M_{21}(M_{24} + M_{22})\dot{\psi}}{n} \quad (28)$$

The design of the yaw motion sliding mode controller is presented as (29):

$$s_2 = c_3\phi + c_4\dot{\phi} \quad (29)$$

By substituting the equations to the robot dynamic, the second input can be calculated as (30):

$$u_6 = \frac{M_{66}\varepsilon_2 sign(s_2)}{-c_4} - f_6 + \dot{\phi}(M_{65} - c_3M_{66}) \quad (30)$$

where:

$$f_2 = MLRx_4^2 \sin x_3 \quad (31)$$

$$f_4 = MgL \sin x_3 + ML^2x_6^2 \sin x_3 \cos x_3 \quad (32)$$

$$f_6 = -2ML^2x_4x_6 \sin x_3 \cos x_3 \quad (33)$$

From Eqs. 34 and 35, the inputs of left and right wheels are:

$$v_r = \frac{RR_m}{nK_tw}u_6 - \frac{R_m}{2nK_t}u_2 \quad (34)$$

$$v_l = -\frac{RR_m}{nK_tw}u_6 - \frac{R_m}{2nK_t}u_2 \quad (35)$$

Figure 6 depicts the block diagram of closed look position control with sliding mode controller for the TWIP.

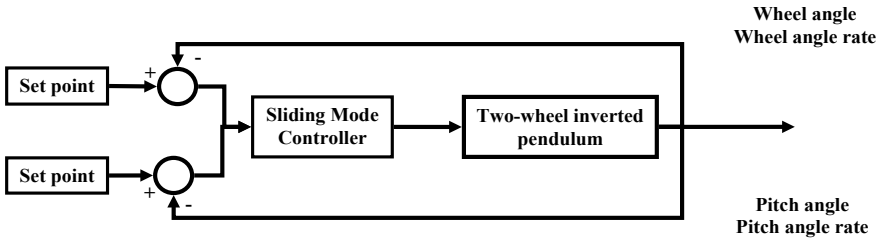

Fig. 6 SMC block diagram for TWIP

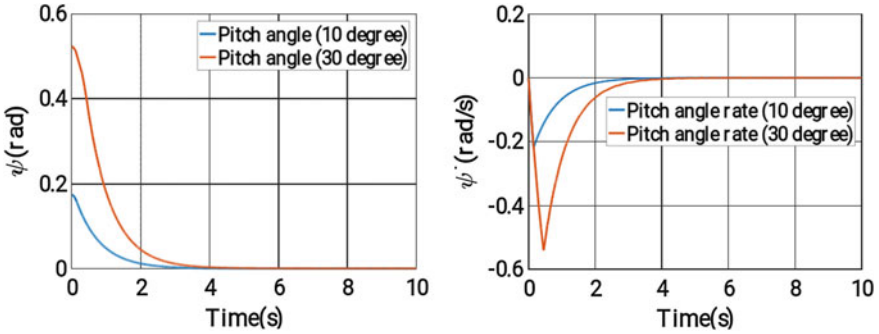

Fig. 7 The pitch angle and its rate of SMC in simulation

Table 4 Transient performance of SFC with LQR and SMC in simulation

	SFC		SMC	
Initial condition	10°	30°	10°	30°
Rise time (s)	0.181	0.166	3.144	4.374
Settling time (s)	2.25	3.04	1.638	2.581
Percentage of overshoot (%)	36.12	38.36	0	0

The angular reaction of the wheels is presented in Fig. 7.

The simulation results are summarized in Table 4. From this table, one can see that the SMC has better transient performance than SFC does in terms of settling time and percent overshoot.

4 Experiments

This TWIP robot is built with four main parts: controller and sensors, gear DC motors, battery, and structure. Arduino Uno is the controller of the TWIP and allows the driver shield to drive gear DC motors. The gear DC motors of the robot could robustly keep the robot stable. The driver shield is L298, which is a dual full-bridge driver. It can transform the real time data from Arduino board to the DC motors. To record the angular position like pitch, yaw and wheel angles, Arduino has been connected to two different sensors. (i.e., IPU 6050 which has accelerometer sensors, gyroscope). As it contains 16-bits analog to digital conversion hardware for each channel, it could be more precise.

In addition, using X-bee shield can wirelessly provide the data transmission to computer. The gear-DC-motors made by Faulhaber with maximum revolution of 350 rpm. Moreover, the power is supplied by Li-Po battery/4000 mA. The diameter of wheels is 108 mm. the center mass of robot is located in the middle of the wheels' axis (Fig. 8).

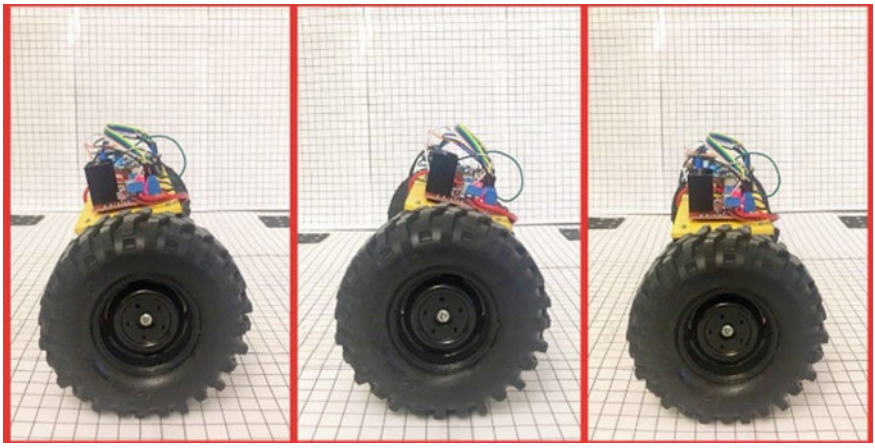

Fig. 8 TWIP robot with different pitch angle

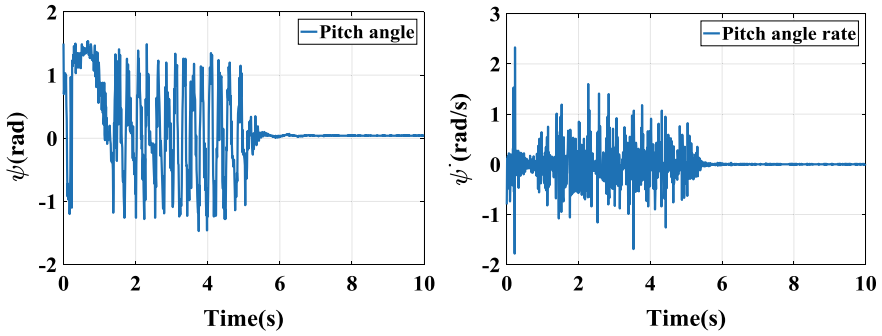

Fig. 9 The experiment results of pitch angle and its rate of PID controller

The experimental results of pitch angle and its rate of PID controller are presented in Fig. 9.

The experimental results of pitch angle and its rate of SFC controller are presented in Fig. 10.

In the next, to evaluate the performance of the sliding mode control, the pitch angle and its rate have been illustrated in Fig. 11.

In both experimental tests, a big push has been applied to the TWIP robot around 1 s to test the disturbance rejection ability of both controllers. From Figs. 9, 10 and 11, one can see that PID, SFC and SMC can recover from the push and achieve self-balancing. However, it only takes SMC less than 2 s to settle in the zero angles position while SFC takes more than 2 s and PID controller takes 6 s to reach the self-balancing state. The video of the experiments is uploaded in Youtube https://youtu.be/EKycX3Wqg9k/ and https://youtu.be/a6w5zxU8IBU. The experi-

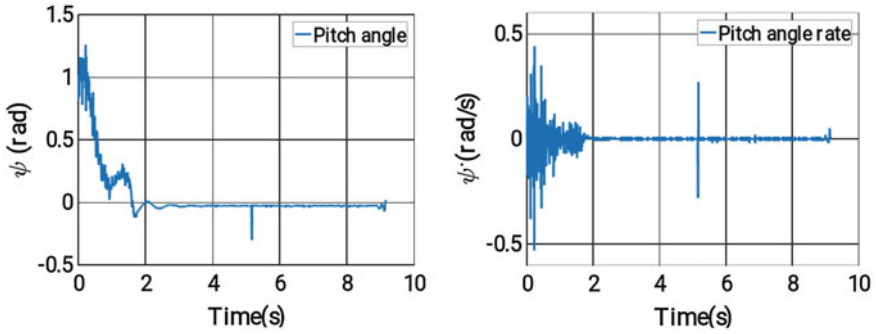

Fig. 10 The experiment results of pitch angle and its rate of SFC

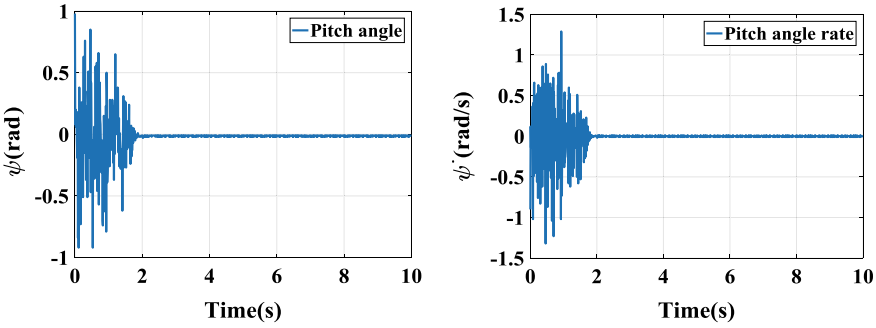

Fig. 11 The experiment results of pitch angle and its rate of SMC

mental tests demonstrate that SMC controller outperforms the PID controller and SFC tuned by LQR.

Table 5 shows the performance comparison among the presented methods, PID, SFC controller and SMC controller designed based on 2-DoF model [14]. As the comparison depicts, the overall performance of the presented SMC is better than those of the other methods. The settling time of the presented SMC illustrates the robot can react faster compared to the SMC methods [14] due to the consideration of 3 degree of freedoms (DoFs) for the dynamical modeling instead of 2 DoF (yaw angle). Although the overshoot of the proposed SMC controller is bigger than the one in [14], the important point which needs to be considered is initial condition. The robot initial angles are remarkably bigger than those set in the SMC controller in [14] to examine the robustness of the controllers. Definitely, the system can respond faster than other methods do with bigger initial conditions because the controller is designed based on 3 DoF nonlinear dynamical model.

Table 5 Summary of performance characteristics in the literature and current study

	SMC [14]	SMC [current study]	LQR [current study]	PID [current study]
Settling time (s)	<4	2	3.1	6
Overshoot (rad)	~0.3 (small initial angels)	1.5 (big initial angles)	1.2 (big initial angles)	0.8 (big initial angles)
Robustness test	No	Very good	Good	Not good

5 Conclusion

In this study, a customer-designed TWIP robot is presented, which is an inherent unstable and nonlinear system. A SMC for balancing and steering movement is designed based on the 3-DoF dynamic model derived by the Lagrangian function method. From simulation results of the PID controller, SFC and SMC for the TWIP system, it can be concluded that the SMC has better transient performance in stabilizing the TWIP robot. To further evaluate the SMC, SFC and PID control performances, experimental tests have been conducted and validated the effectiveness of the design of the robot. As it is presented in the aforementioned test results, the settling time of SMC is three times shorter than that of PID controller. The performances of SMC is superior to those of SFC and SMC in [14] in terms of settling time and robustness. The future work includes the further improvement of control performances considering the actuation constraints.

References

1. Nasir ANK, Ahmad MA, Ismail RR (2010) The control of a highly nonlinear two-wheels balancing robot: A comparative assessment between LQR and PID-PID control schemes. World Acad Sci Eng Technol 70:227–232
2. Marzi H (2006) Fuzzy control of an inverted pendulum using AC induction motor actuator. In: Proceedings of IEEE international conference on computational intelligence for measurement systems and applications. IEEE, July 2006
3. Tsai CC, Ju SY, Hsieh SM (2010) Trajectory tracking of a self-balancing two-wheeled robot using backstepping sliding-mode control and fuzzy basis function networks. In: Proceedings of IEEE/RSJ international conference on intelligent robots and systems (IROS). IEEE, October 2010
4. Unluturk A, Aydogdu O (2017) Adaptive control of two-wheeled mobile balance robot capable to adapt different surfaces using a novel artificial neural network–based real-time switching dynamic controller. Int J Adv Rob Syst 14(2):1729881417700893
5. Villacres J, Viscaino M, Herrera M et al (2016) Controllers comparison to stabilize a two-wheeled inverted pendulum: PID, LQR and sliding mode control. Moment 2(2):12
6. Gans NR, Hutchinson SA (2006) Visual servo velocity and pose control of a wheeled inverted pendulum through partial-feedback linearization. In: Proceedings of IEEE/RSJ international conference on intelligent robots and systems. IEEE, October 2006

7. ul Hasan M, Hasan KM, Asad MU et al (2014) Design and experimental evaluation of a state feedback controller for two wheeled balancing robot. In: IEEE 17th international multi-topic conference (INMIC). IEEE, December 2014
8. Chen ML (2012) Analysis and design of robust feedback control systems for a nonlinear two-wheel inverted pendulum system. In: Proceedings of international symposium on computer, consumer and control. IEEE, June 2012
9. Nomura T, Kitsuka Y, Suemitsu H et al (2009). Adaptive backstepping control for a two-wheeled autonomous robot. In: Proceedings of ICCAS-SICE. IEEE, August 2009
10. Pathak K, Franch J, Agrawal SK (2005) Velocity and position control of a wheeled inverted pendulum by partial feedback linearization. IEEE Trans Rob 21(3):505–513
11. Pathak K, Franch J, Agrawal SK (2004) Velocity control of a wheeled inverted pendulum by partial feedback linearization. In: Proceedings of 43rd IEEE conference on decision and control. IEEE, December 2004
12. Huang J, Guan ZH, Matsuno T et al (2010) Sliding-mode velocity control of mobile-wheeled inverted-pendulum systems. IEEE Trans Rob 26(4):750–758
13. Yue M, Sun X, Li N et al (2015) Dynamic motion planning and adaptive tracking control for a class of two-wheeled autonomous vehicle with an underactuated pendular suspension. J Dyn Syst Meas Contr 137(10):101006
14. Zhang Z, Li L (2016) Design and implementation of two-wheeled mobile robot by variable structure sliding mode control. In: Proceedings of 35th Chinese control conference (CCC). IEEE, July 2016
15. Esmaeili N, Alfi A, Khosravi H (2017) Balancing and trajectory tracking of two-wheeled mobile robot using backstepping sliding mode control: design and experiments. J Intell Rob Syst 87(3–4):601–613
16. Lv W, Kang Y, Zhao P (2013) Speed and orientation control of a two-coaxial-wheeled inverted pendulum. In: Proceedings of 32nd Chinese control conference (CCC). IEEE, July 2013
17. Dai F, Gao X, Jiang S et al (2015) A two-wheeled inverted pendulum robot with friction compensation. Mechatronics 30:116–125
18. Thao NGM, Nghia DH, Phuc NH (2010). A PID backstepping controller for two-wheeled self-balancing robot. In: International forum on strategic technology (IFOST). IEEE, October 2010
19. Velazquez M, Cruz D, Garcia S et al (2016) Velocity and motion control of a self-balancing vehicle based on a cascade control strategy. Int J Adv Rob Syst 13(3):106